

Multi-focus Image Fusion Algorithm Based on Multilevel Morphological Component Analysis

Lingling Wang^{1, a}, Xiongfei Li^{2, b}

¹ College of Computer Science and Technology, Jilin University, Changchun 130012, China.

² Key Laboratory of Symbol Computation and Knowledge Engineer of Ministry of Education, Jilin University, Changchun 130012, China.

^a251200993@qq.com, ^bxiongfei@jlu.edu.cn

Keywords: multilevel morphological component analysis; multi-focus image fusion; feature vectors; weighted fusion rules.

Abstract. This study proposed a novel image fusion algorithm based on weighed multilevel morphological component analysis (FWMMCA). First, morphological component analysis is improved into a new multi-scale decomposition algorithm—multilevel morphological component analysis (MMCA). Then, feature vectors are extracted from MMCA sub images, which are used to reflect brightness, texture regularity, energy, and randomness of those images. Moreover, the feature vectors are innovatively used as weight in fusion rules, to propose a weighted fusion rules. Sub images are fused via those fusion rules, which are finally reconstituted into fused image.

Introduction

When it comes to vision-related processing tasks, such as stereo matching, edge detection and image segmentation, it is very important that all the objects in the scene should be clear. However, it may not be always feasible for the optical imaging system because of the limitation of the depth of field. The most common and effective alternative is image fusion. Generally, image fusion methods can be classified into two categories: (1) spatial domain based methods, and (2) transform domain based methods.

Spatial domain based methods share similar problem: block artifacts. Transform domain based methods include pyramid-based fusion methods and Discrete wavelet transform (DWT) based method. As Discrete wavelet transform (DWT) can get directional information, it is superior to those pyramid-based ones[1] when fusing images. But DWT-based-method still has common problems of the wavelet-based fusion algorithm, such as shift variance.

Starck proposed morphological component analysis (MCA) relies on two principles: morphological diversity and sparseness [2]. Sparseness ensures most of the signal falls on the axis of representation spaces, which provides MCA with orthogonality and shift invariance, make MCA superior to wavelet algorithm in image decomposition field. However, classical MCA can only decompose each image into two parts: smooth one and textural one. It tends to result in under-decomposition for image fusion, and makes it difficult to design fusion rules.

Fusion scheme of FWMMCA

Step1. Use MMCA to decompose source images into multi scale space, the output are sub images.

Step2. Extracting feature vectors from those sub images.

Step3. Use the feature vectors as weight in fusion rules, to propose a weighted fusion rules.

Step4. Fuse the sub images via those fusion rules, which are finally reconstituted into fused image.

The general framework of the FWMMCA is shown in Fig. 1 as follows:

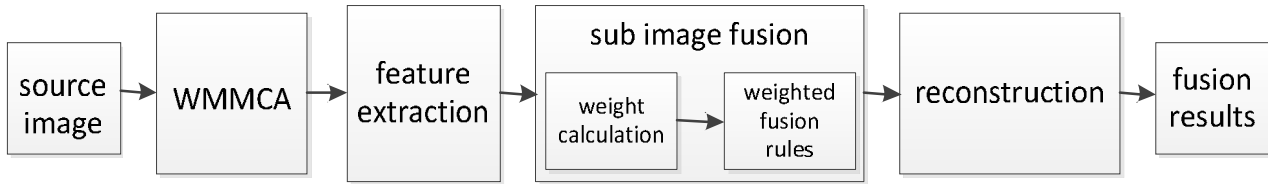


Fig1. Fusion algorithm based on weighed multilevel morphological component analysis

Multilevel Morphological Component Analysis

The normal MCA expressed the source image as a linear combination: texture part S_t and nature part S_n , namely $S = S_t + S_n$. And the decomposition process of source image is transformed into the process of solving formula(1).

$$\{\alpha_n^{opt}, \alpha_t^{opt}\} = \arg \min_{\{\alpha_n, \alpha_t\}} (\|\alpha_n\|_0 + \|\alpha_t\|_0), \quad \text{subject to } S = \Phi_n \alpha_n + \Phi_t \alpha_t. \quad (1)$$

In practical, we can find that sparsity causes MCA only sparate a few texture information from the nature one, and the smooth layer is over preserved. Considering this unbalance decomposition is not conducive to the preservation of the texture of source images. Since nature part has more information, we improve the linear assumptions of MCA into iterative assumptions to propose MMCA, as shown in (2).

$$S = S_{i0} + (S_{i1} + (S_{i2} + (\dots (S_{iK} + S_{nK})))) \quad (2)$$

By replacing source image with nature layer image obtained from last iteration, we can get a set of nature-texture pair $(S_{i0}, S_{i1}, S_{i2}, \dots, S_{iK}, S_{nK})$, K is the number of levers during MMCA decomposition. The proposed multilevel morphological component analysis algorithm is implemented as follows

1. Initial iteration number $K, S_i = S, i = 0, S$ is one of the source images.
2. When $i < K$, Perform the following iteration process:
 - ① Initial iteration number $Q(Q$ is the maximum length of coefficient vector α), Set threshold $\delta = \lambda \cdot Q$.
 - ② The iterative process with threshold is implemented as follows :
 - Part A. Assume S_{ii} is constant, update S_{ni} : Calculating residual quantity $R = S_i - S_{ii}$, Calculating $\alpha_n = T_n^+ R$, Processing α_n coefficient via soft-threshold method with threshold δ , get coefficient α'_n . Reconstruct $S_n, S_n = T_n \alpha'_n$.
 - Part B. Assume S_{ni} is constant, update S_{ti} : Calculating residual quantity $R = S_i - S_{ni}$, Calculating $\alpha_t = T_t^+ R$, Processing α_t coefficient via soft-threshold method with threshold δ , get coefficient α'_t . Reconstruct $S_t, S_t = T_t \alpha'_t$.
 - Part C. Update threshold $\delta = \delta - \lambda$.
 - Part D. If $\delta \geq \lambda$, return to ②, otherwise execute ③.
 - ③ Update $S_{i+1} = S_{ni}$ and $i = i + 1$.

Fig.2 shows a set of decomposition result. To compare the decomposition results of MMCA with the decomposition results of MCA, the former decomposition method get more smooth nature layer and more soft edges, which means MMCA decompose more texture information from the source image.

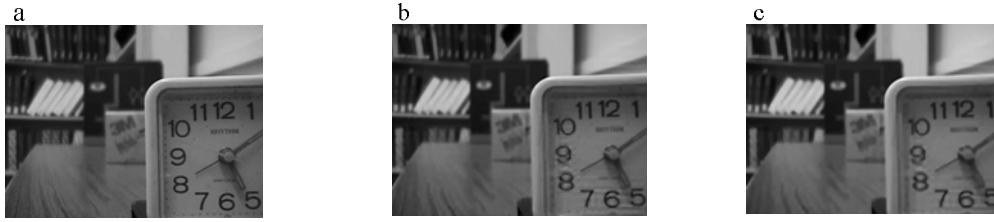


Fig.2 Decomposition results of MMCA and MCA: (a) the source image; (b) the nature sub image (MCA); (c) the nature sub image (MMCA)

Feature Extraction

The four features of the pixel at position (x, y) are calculated as following equation in Table 1. The value of g varies with the position of current pixel in sub image: $g=4$ for the corner, $g=6$ for the edge, and $g=9$ for other position in sub images. $p(x, y)$ is pixel value at position (x, y) , and $h^\mu(x, y)$ is the μ -th value in the normalized histogram of absolute values of sub image in the $3*3$ local window at position (x, y) .

Table1 Feature formulas of the center pixel

| Features | Moments | Expressions | Measures |
|-----------------|-----------------|---|-----------------------|
| FS ₁ | Mean | $\frac{1}{g} \sum_{m=-1}^1 \sum_{n=-1}^1 p(x+m, y+n) $ | Luminance |
| FS ₂ | Mean of square | $\frac{1}{g} \sum_{m=-1}^1 \sum_{n=-1}^1 p(x+m, y+n) ^2$ | Regularity of texture |
| FS ₃ | Variance | $\frac{1}{g} \sum_{m=-1}^1 \sum_{n=-1}^1 p(x+m, y+n) - FS_1 ^2$ | Energy and smoothness |
| FS ₄ | Shannon entropy | $\sum_{\mu=0}^{255} h^\mu(x, y) \times \log_2 \left(\frac{1}{h^\mu(x, y)} \right)$ | Randomness |

Texture Part Fusion Rules

Texture coefficients are determined by selecting maximum absolute values based on the features vector sets of each layer. The \mathbf{l} -th texture sub-image's coefficient at position (x, y) is calculated as follows:

$$p_{\mathbf{l}}^F(x, y) = R * p_{\mathbf{l}}^A(x, y) + (1 - R) * p_{\mathbf{l}}^B(x, y), \quad \text{subject to :}$$

$$R = \begin{cases} 1, & \text{if } \left| \sum_{i=1}^4 FS_{\mathbf{l}}^A(i) \right| \geq \left| \sum_{i=1}^4 FS_{\mathbf{l}}^B(i) \right| \\ 0, & \text{if } \left| \sum_{i=1}^4 FS_{\mathbf{l}}^A(i) \right| < \left| \sum_{i=1}^4 FS_{\mathbf{l}}^B(i) \right| \end{cases} \quad (\mathbf{l} = 1, 2, 3, \dots, L) \quad (3)$$

Nature Part Fusion Rules

The feature vectors are innovatively used as weight in fusion rules, The nature part fusion rule is explained as below:

$$p_n^F(x, y) = \frac{\left(\sum_{i=1}^4 FS_n^A(i) \right) * p_n^A(x, y) + \left(\sum_{i=1}^4 FS_n^B(i) \right) * p_n^B(x, y)}{\sum_{i=1}^4 FS_n^A(i) + \sum_{i=1}^4 FS_n^B(i)} \quad (4)$$

Experiments and result analysis

To verify the superiority of the proposed fusion method, we compare it with five other fusion algorithms, including Gradient Pyramid based algorithm (GRP) [3], Morphological Pyramid based algorithm (MP) [4], Hierarchical Pyramid based algorithm (FSD) [5], and Discrete Wavelet Transform based algorithm (DWT) [6]. The decomposition level in GRP, MP, FSD and DWT is 6. The proposed algorithm was implemented on MATLAB 2009b, and the decomposition level of MMCA is 3.

Five different objective measures including Mutual Information (MI) [7], Peak Signal to Noise Ratio (PSNR) [8], Structural Similarity (SSIM) [9], and Piella's metrics (Q , Q_w) [10] are used to evaluate the performance of the fusion algorithms. The experiment results of image "plants" are shown in Fig.3. And objective evaluation of three pictures are listed in Table 2. The highest scores have been marked in bold and the second high in those scores marked in italics.



Fig 3. Resultant images fused by those five algorithms: "plants"

Table 2 Evaluation of different fusion schemes

| Images | Measures | GRP | MP | FSD | DWT | FWMMCA |
|--------------|----------------------|---------|---------|---------|----------------|----------------|
| (1) plants | <i>MI</i> | 5.3950 | 5.4825 | 5.2450 | 6.0308 | 6.3009 |
| | <i>PSNR</i> | 24.729 | 23.652 | 24.700 | 26.952 | 27.000 |
| | <i>SSIM</i> | 0.89217 | 0.8614 | 0.88971 | 0.89433 | 0.89829 |
| | <i>Q</i> | 0.87912 | 0.84764 | 0.87335 | 0.89893 | <i>0.89732</i> |
| | <i>Q_w</i> | 0.88912 | 0.87703 | 0.88648 | 0.90751 | 0.91370 |
| (2) calendar | <i>MI</i> | 4.7412 | 5.1525 | 4.7168 | 5.1803 | 5.1930 |
| | <i>PSNR</i> | 24.2370 | 23.7070 | 24.1960 | 26.7930 | 26.9390 |
| | <i>SSIM</i> | 0.8035 | 0.7950 | 0.8015 | 0.8270 | 0.8270 |
| | <i>Q</i> | 0.7665 | 0.7733 | 0.7635 | 0.7888 | 0.7907 |
| | <i>Q_w</i> | 0.8100 | 0.8105 | 0.8076 | 0.8362 | <i>0.8113</i> |
| (3) leopard | <i>MI</i> | 6.0788 | 7.1585 | 5.9580 | 7.1940 | 7.4495 |
| | <i>PSNR</i> | 22.7810 | 24.2390 | 22.7280 | 26.7560 | 30.0200 |
| | <i>SSIM</i> | 0.8481 | 0.9128 | 0.8459 | 0.9343 | 0.9399 |
| | <i>Q</i> | 0.8273 | 0.9017 | 0.8281 | 0.8899 | 0.9570 |
| | <i>Q_w</i> | 0.8838 | 0.8926 | 0.8824 | 0.9293 | <i>0.9281</i> |

Experiments show that the proposed FWMMCA has outstanding performance in multi-focus image fusion in terms of subjective and objective evaluation. The fusion result of FWMMCA didn't appear gray distortion, and preserve the structure and details of the source images well. The objective evaluation results are in line with the subjective judgments mentioned above.

Conclusions

This study puts forward a new multi-focus image fusion method based on improvements of MCA and feature extraction. The feature vectors of sub images are innovatively used as weight in fusion rules, to propose a weighted fusion rules. The results of theory analysis and simulation experiments showed that the proposed algorithm can get a better fusion result than comparison algorithms.

Acknowledgements

This work was financially supported by National Science Foundation of China (61272209) and Agreement of Science & Technology Development Project, Jilin Province (20150101014JC).

References

- [1] Pajares G, and De La Cruz J M. A wavelet-based image fusion tutorial. *Pattern recognition*, 37(9) (2004) 1855-1872.
- [2] Starck J L, Elad M, and Donoho D L. Image decomposition via the combination of sparse representations and a variational approach. *Image Processing*, 14(10) (2005) 1570-1582.
- [3] Burt P J, and Kolczynski R J. Enhanced image capture through fusion. *Computer Vision: Fourth International Conference on IEEE*, (1993) 173-182.
- [4] Matsopoulos G K, Marshall S, and Brunt J N H. Multiresolution morphological fusion of MR and CT images of the human brain. *Image and Signal Processing*, 14(3) (1994) 137-142.
- [5] Anderson, C.H. Filter-subtract-decimate hierarchical pyramid signal analyzing and synthesizing technique. U.S. Patent and Trademark Office. (1988).
- [6] Pajares G and De La Cruz J M. A wavelet-based image fusion tutorial. *Pattern recognition*, 37(9) (2004) 1855-1872.
- [7] Qu G, Zhang D, and Yan P. Information measure for performance of image fusion. *Electronics letters*, 38(7) (2002) 313-315.
- [8] Huynh-Thu Q and Ghanbari M. Scope of validity of PSNR in image/video quality assessment. *Electronics letters*, 44(13) (2008) 800-801.
- [9] Wang, Z., Simoncelli, E. P., and Bovik, A. C.. Multiscale structural similarity for image quality assessment. In *Signals, Systems and Computers, 2004. Conference Record of the Thirty-Seventh Asilomar Conference on Vol. 2(2003)*, p. 1398-1402.
- [10] Piella G and Heijmans H. A new quality metric for image fusion. *Image Processing: 2003 International Conference on IEEE*, 3 (2003) III-173-176.